

HEAT LOAD ANALYSIS OF 3 TESLA WIGGLER IN CANDLE STORAGE RING

S Tunyan, M Aghasyan, V Avagyan, M Ivanyan
Center for the Advancement of Natural Discoveries using Light Emission
Acharian 31 - 375040 Yerevan - Armenia

Abstract

In order to expand the CANDLE radiation capability in hard X-ray region, it is foreseen to install 3 Tesla wiggler for the X-Ray imaging beamline at CANDLE. Its design will be mainly based on a 3 Tesla permanent magnet wiggler designed and assembled at ESRF [1]. In this report we present the study of the vacuum chamber thermal loading caused by the installation of similar wiggler with 10 periods. The analysis has enabled to determine the position and construction of the absorbers providing possibility to use similar critical Insertion Devices (ID) in future.

1. Introduction

Centre for the Advancement of Natural Discoveries using Light Emission (CANDLE) is a project of third generation synchrotron light source that provides high brilliance X-ray beams for scientific research. The need for a light source with higher radiation intensity and critical energy requires the utilization of insertion devices with higher field strengths. In order to expand the CANDLE radiation capability in hard X-ray region, it is foreseen to install 3 Tesla wiggler for the X-Ray imaging beamline at CANDLE [2]. Its design will be mainly based on 3 Tesla permanent magnet wiggler designed and assembled at ESRF. Similar wiggler, but with 10 periods, will be a type of device at CANDLE, which achieves wide beam fan and maximum peak flux density that can serve more than one beamline. On the other hand, such increases of the period number will expand the beam horizontal size up to critical concerning the aperture of the storage ring vacuum chamber. In this report we present the study of the vacuum chamber thermal loading caused by the installation of similar wiggler, thereby determining capability of vacuum chamber in relation to ID Synchrotron Light (SL) emission.

2. 3 Tesla Wiggler Characteristics

The radiation of SL from insertion devices depends on the type of device and machine parameters. The 3T wiggler and storage ring main parameters are listed in Table 1. 3 Tesla multipole Wiggler with 10 periods, length of each 21.8 cm, will deliver photon beam with a critical energy of 17.95 keV. The gap opening to achieve this critical energy is 11 mm. The total power of radiation beam is about 39.1 kW. This is about 4 times greater than the power emitted by one CANDLE bending magnet.

Table 1. Storage ring and 3T Wiggler parameters.

Maximum Beam Current	350 mA
Maximum Beam Energy	3.0 GeV
Wiggler Magnetic Field	3.0 T
Wiggler Number of Periods	10
Wiggler Period Length	21.8 cm
Beam Critical Energy	17.95 KeV
Wiggler Gap	11 mm
Beam Total Power	39.1 kW
Wiggler Deflection Parameter	61
Beam Peak Power Density	9.2 kW/mr ²

The power density is also much greater: its peak reaches about 9.2 kW/mrad². The photon beam power density profile is shown in Fig.1. The spatial distribution of beam from wiggler has a complex profile, Gaussian in the vertical plane and parabolic in the horizontal direction. The fan of radiation from 3T wiggler is about 20.8 mrad in the horizontal plane, and of the order of 0.34 mrad in the vertical direction. The maximum total power and the beam horizontal opening of this critical insertion device are very high, that forces us, already on the current project stage, to carry out more detailed pre-analysis of power distribution in the storage ring, as well as to consider possible consequences concerning vacuum chamber walls, which will be made of stainless steel.

The CANDLE storage ring lattice consists of 16 identical Double-Bend Achromatic (DBA) cells, 13 of which have an opportunity to install IDs. One of such ID photon beam emission tract is shown schematically on Fig.2. The first 6-inch exit port in each cell, mounted on ID radiation emission axis, should provide outlet of radiation power, generated by IDs, from the storage ring vacuum chamber. The both absorbers located near the exit port will be used to protect vacuum chamber walls from radiation of bending magnets. In principle, for the horizontal emission fan of 3T Wiggler, there is an opening of about 67 mm on either side of the central line at the end of the vacuum chamber (at the distance of 6.44 m from the center of the straight section). Such an angular opening from the center of the straight section is rather conformed to the exit aperture of the vacuum chamber (70 mm on either side). Moreover, taking into account the use of an interlock system that will abort the electron beam at a significant deviation from a design orbit, we could avoid additional protection (the matter concerns distributive absorber) of vacuum chamber walls. However, at the detailed analysis, as it will be obvious below, the synchrotron light of the critical insertion device similar to 3T Wiggler, can leave a trace onto the storage ring vacuum chamber walls, even so without miss-steering.

In principle, this problem can be solved after the installation of main vacuum chamber. The beam's tails can be dissected at the end of the straight section, as usually made in other centers. But some reasons induced us to install distributive absorber along the vacuum chamber wall in each cell, thereby increasing the vacuum chamber ability in relation to ID SL emission.

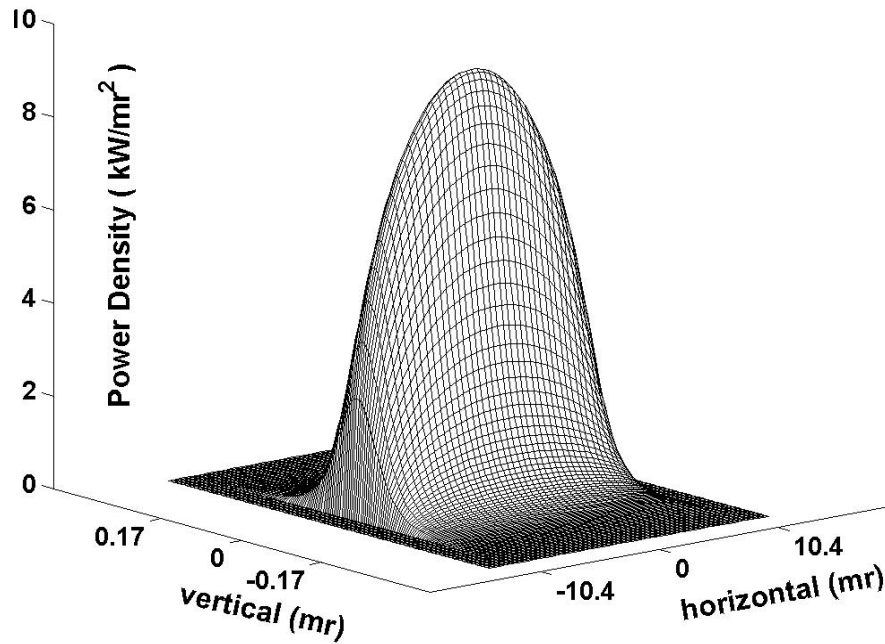


Fig. 1. 3T Wiggler beam power density distribution.

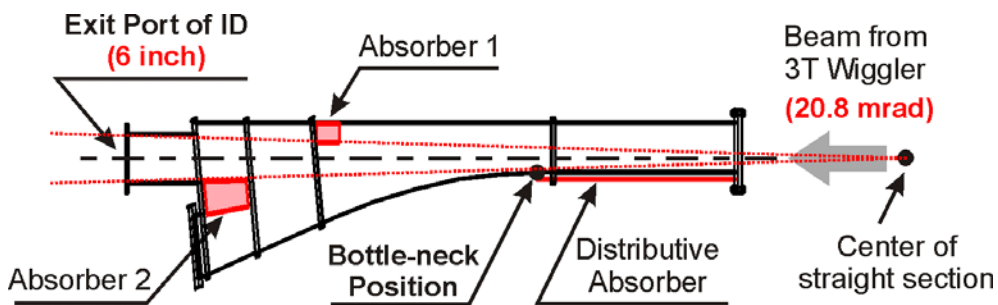


Fig. 2. SL emission tract of ID in CANDLE storage ring.

3. Evaluation Process of Heat Load

While solving the problem of thermal loading on vacuum chamber caused by the 3T wiggler, we were interested basically in two parameters: fan horizontal opening and beam power density. We were based on the well-known formula for the distribution of radiated power from an electron in a sinusoidal trajectory, which applies with reasonable approximation to undulators and, to a lesser extent, wigglers [3]:

$$\frac{dP}{d\theta d\psi} = P \frac{21\gamma^2}{16\pi K} G(K) f_k(\gamma\theta, \gamma\psi)$$

where P is the total (angle-integrated) radiated power, γ is Lorenz relativistic factor, K is the deflection parameter of device. The function $G(K)$ tends to unit at large K , as in our case.

The

$f_k(\gamma\theta, \gamma\psi)$ is the angular distribution function, which is normalized as $f_k(0,0) = 1$. The angular distribution function can be expressed in the integral form and best evaluated numerically:

$$f_k(\theta, \psi) = \frac{16K}{7\pi G(K)} \int_{-\pi}^{\pi} \sin^2 \alpha \left[\frac{1}{D^3} - \frac{4(\gamma\theta - K \cos \alpha)^2}{D^5} \right] d\alpha$$

where $D = 1 + (\gamma\psi)^2 + (\gamma\theta - K \sin \alpha)^2$ and $\alpha = 2\pi Z/\lambda$, $0 \leq Z \leq N\lambda$ ($N\lambda$ -wiggler length). Subintegral expression of angular distribution function depends strongly on magnetically structure, and at the transition to Cartesian coordinates requires the account of design distance. The high value of the deflection parameter and short design distance have induced us to consider this multipole wiggler both as a single whole device, and as a system of separate sources. At the second assumption this equation will be operated on each local source and for each different distance and superposition method will be applied for the completed solution, as illustrated in Fig. 3.

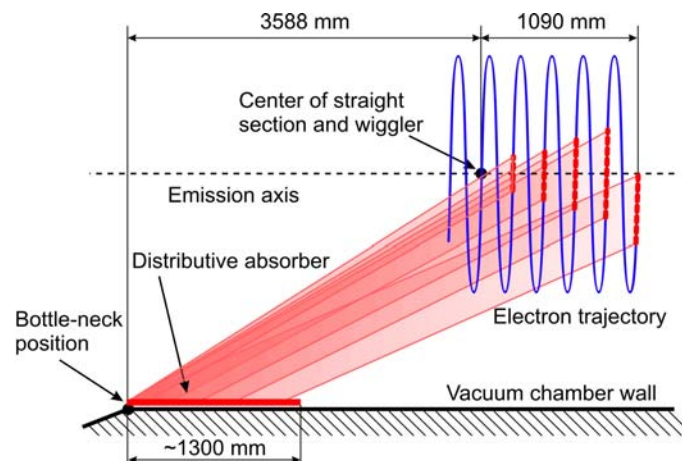


Fig. 3. Target setting of heat load evaluation.

Correctness of the second assumption should be beyond question, as in the case $K \gg 1$ the radiation emitted in the poles of the wiggler is incoherently superimposed and interference effects are less important [4]. All calculations of the above-stated parameters of the 3T Wiggler, as well as sequent reasons are made according to the first assumption. In the second case other results have been obtained. As well as in the first consideration, it is assumed that the center of the separate sources system coincides with the center of vacuum chamber straight section. Thus the first radiation source of 3T Wiggler should be considered on distance $\lambda N/2$ from the center of straight section up-stream. This source sets the maximal synchrotron light deviation of the whole device system. The subsequent analysis shown, that in the zone of radiation, interesting for us, the difference of power density distribution between these two settings is significant (see Fig.4). Taking as a basis the second case, it can be prescribed, that some part of radiation power is dissected on walls of the vacuum chamber, both on the right and on the left. We suggest paying special attention to the photon Absorber 1 (see Fig.2), located at the exit of the photon beam of similar critical insertion devices. It also should be noted that the area of the vacuum chamber near Position Bottle-neck can run the risk to be attacked by photon beam from the 3T Wiggler. The last statement has compelled to install distributive absorber in this zone.

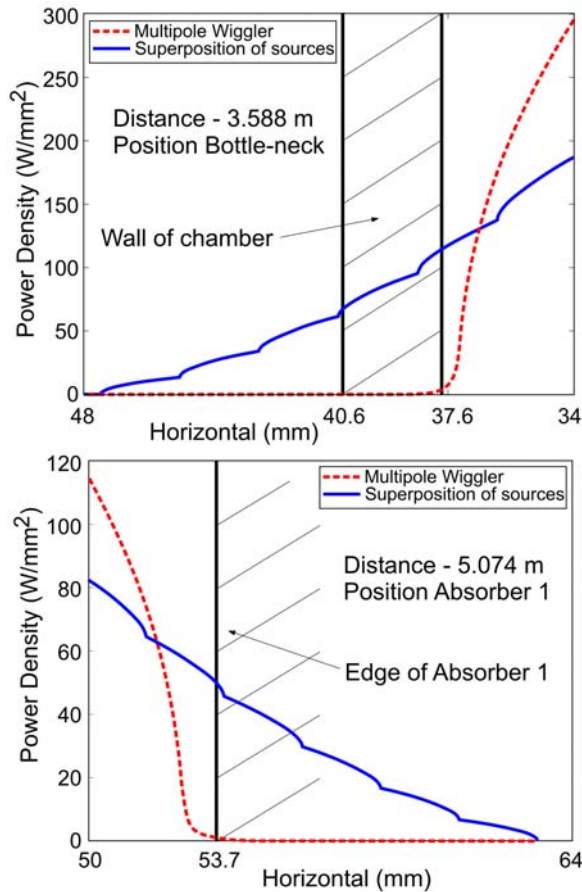


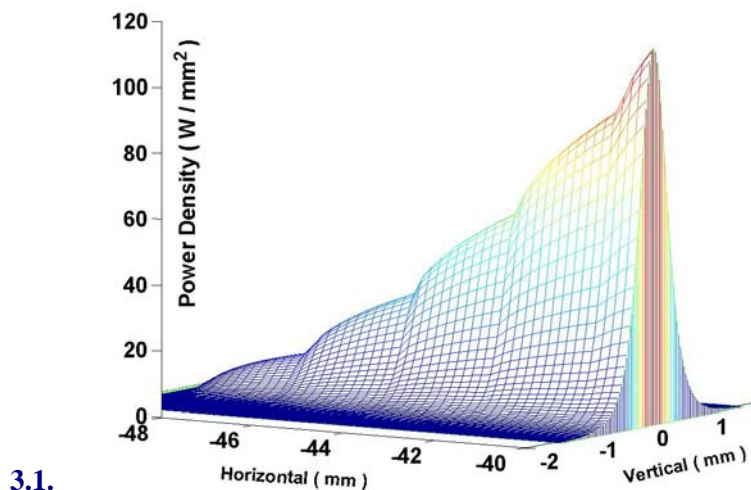
Fig. 4. Horizontal power density distribution of 3T Wiggler.

4. Thermal Load

The thermal load in these regions depends on the source distance and on the level of miss-steering. In its turn, the definition of the real level of miss-steering is an intricate problem. But on this stage an attempt to estimate the values of thermal load on absorbers at the reasonable levels of electron bunch deviation from the design orbit has been made. At calculation of thermal loading on photon absorbers, the superposition method has been applied. The matrix superposition of power density values, reinforced by each separate source, revealed spatial distribution of thermal loading in the impact area. As evident in Figure 5, the radiation of first five sources is allocated on distributive absorber. The same profile of power density is allocated on Absorber 1. The peak power density values on these absorbers, at normal angle incidence, are shown in Table 2.

Table 2. Peak power density on absorbers (W/mm^2).

Offset orbit	Absorber 1	Distributive Absorber
none	46	126
0.32mm	50	131
1.0mm	56	150
1.8mm	61	166



3.1.

Fig. 5. Spatial power density profile of 3T Wiggler on Distributive Absorber.

5. Finite Element Modeling and Thermal Analysis

One of the problems while using Finite Element Modeling is to define boundary conditions. The main parameters are heat load distribution and film convection coefficient. The heat load on the absorbers surface depends on the beam power density distribution, taking into account the angle incident. It was already marked, that X-ray beam from wiggler has a complex profile. In order to use the closed form solution we have to fit the beam power, which strikes absorbers, to a Gaussian-distributed heat flux in vertical plane and parabolic-distribution in horizontal plane. Values of heat flux parameters, taking into consideration the angle incident on the absorbers, are shown in Table 3.

Table 3. Heat flux 3T Wiggler parameters on absorbers.

Absorbers	Peak Power Density (W/mm ²)	Height of Fan (mm)	Width of Fan (mm)
Absorber 1	5.3	23.5	11
Distributive Absorber	1.66	1.58	12.6

Besides, each of these absorbers has some nuances, demanding additional attention. Distributive absorber, length of about 1.2 meters, represents a 7 mm thick copper plate brazed on the inner side of the stainless steel vacuum chamber, and a water cooling copper tube will be brazed on the outside of the vacuum chamber. Practically sliding shade (about 0.6°) of radiation allows to reduce power density in 100 times. The narrow flux (1.6mm) is parabolically distributed along the full length, achieving a maximum on the end of the absorber.

The crotch type Absorber 1, located in front of the insertion devices radiation exit ports, on the full width is exposed to thermal loading generated by bending magnet. The radiation generated by 3T Wiggler strikes only the edge of the Absorber 1, but with higher density. The absorption surface is inclined to the incident beam by approximately 5°, thus reducing the incident power density in 10 times. In addition, 1.5-mm-deep external surface fins are used to split the beam footprint into two parts. Asymmetrical water channels and internal fins have allowed to increase film convection coefficient in the basic impact zone. In the present design the Dittus and Boelter relation has been used to define the film convection coefficient [5].

The thermal analysis of presented absorbers has been performed by creating 3-Dimensional model and solving maximum temperature on absorber impact surface and on water channel wall. Software FEMLAB 2.3 has been used to achieve this target. Results of maximum temperatures of the absorbers bottom surfaces, as well as of the cooled walls and main parameters of the models are shown below (Fig.6).

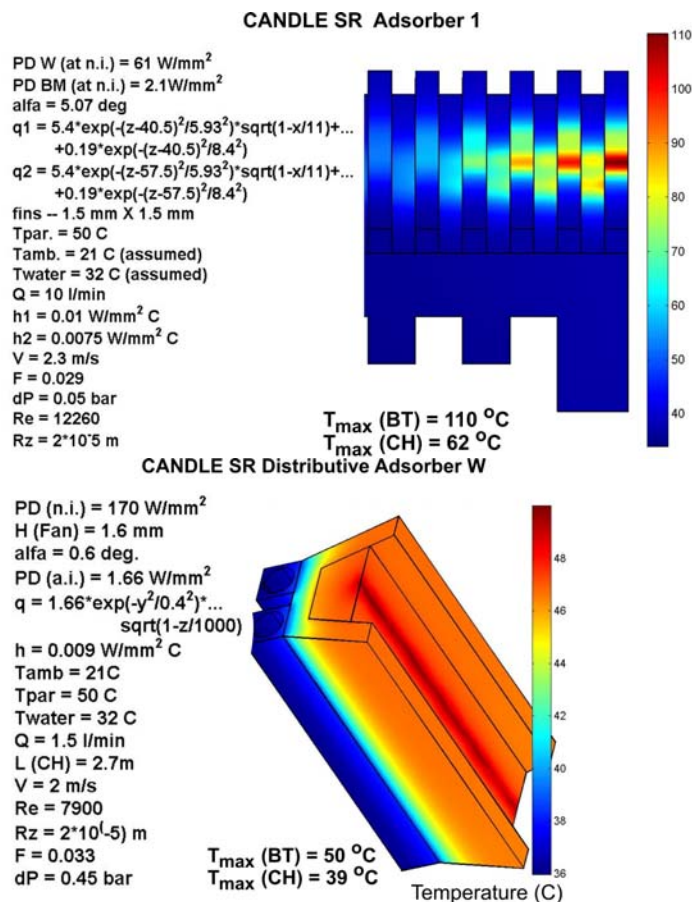


Fig. 6. Storage ring absorbers design.

6. Conclusions

Detailed analysis of power distribution generated by insertion device (in the worst case) in CANDLE storage ring has been carried out. Thermal load profile and values on two absorbers of the storage ring vacuum chambers are determined and calculated. Finite element analysis shows that the temperature due to heat load generated by 3 Tesla permanent multipole wiggler is significantly smaller than the maximum permissible limit [6, 7, 8].

It is necessary to note that consideration of the material thermal stress analysis is absent in this study; it's of no interest for presented absorbers. Such analysis will exist in future, when photon shutter and splitter for this wiggler will be worked-out.

7. Acknowledgements

We would like to thank all the people from the CANDLE team for valuable discussions. Editing of this paper by Ms. Nana Abrahamyan is also sincerely valued.

8. References

- [1] J. Chavanne, P. Van Vaerenbergh and P. Elleaume, A 3 T asymmetric permanent magnet wiggler, NIM A 421 (1999) 352-360.
- [2] Candle Activity Report, Machine Study, 2001-2003.
- [3] S. L. Hulbert and G. P. Williams, Synchrotron Radiation Sources, BNL, Upton, New York, USA, July 1998.
- [4] Volker Saile, Properties of Synchrotron Radiation, IMT, FK GmbH, UK, Karlsruhe, Germany.
- [5] W. Rohsenow, J. Hartnett, E. Ganic, Handbook of Heat Transfer Fundamentals, 2nd Ed., McGraw-Hill, New York, 1985.
- [6] L. Zhang, J. C. Biasci, B. Plan. ESRF Thermal Absorbers: Temperature, Stress and Material Criteria. MEDSI02, 2002.
- [7] Asu Alp, Thermal-Stress Analysis of the High Heat-Load Crotch Absorber at the APS, MEDSI02, 2002.
- [8] S. Sharma, E. Rotela and A. Barcicowski, High Heat-Load Absorbers for the APS Storage Ring, MEDSI2000, 2000